**Tecnologia/Technology**

# EXPERIMENTAL STUDY OF THE PRESSURE DROP OF THE ECOFLUID R1234YF COMPARED TO THE FLUID R134A IN SMOOTH TUBES WITH 4.8MM INTERNAL DIAMMETER

**R. P. Mendes[a],**

**D. L. Pottie[a],**

**L. V. S. Martins[a],**

**J. J. G. Pabon[b]**

**and L. Machado[c]**

[a]Post Graduate Program of Federal Univesity of Minas Gerais

Departament of Mechanical Engineering

Av. Antônio Carlos, 6627

CEP. 31270-901, Belo Horizonte, Minas Gerais, Brasil

ramondepaoli@yahoo.com.br

dpottie@gmail.com

leo.vsm@hotmail.com

luizm@demec.ufmg.br

[b]Federal University of Itajubá

Department of Mechanical Engineering

Av. B. P. S., 1303

CEP. 37500-015, Itajubá, Minas Gerais, Brasil

jjgp@unifei.edu.br

**ABSTRACT**

The refrigerant fluid R1234yf is a hydrofluorefine with zero potential for degradation of the ozone layer and low potential for global warming. It is one of the potential substitutes for the currently used R134a in automotive systems. In this work, the pressure drop suffered by the fluids R134a and R1234yf when flowing in a test section through a pipe with a 4.8 mm internal diameter was measured. The pressure drop was plotted as a function of the void fraction at the exit of the test section and the values were compared concerning the change in mass flux, change in saturation temperature, and comparatively between R1234yf and R134a. A significant increase in pressure drop was observed by the increases of the mass flux, showing an increment of 155.46% of the pressure loss from 200 to 300 $kg \cdot m^{-2} \cdot s^{-1}$ for R1234yf at 35ºC and 161.07% for R134a in the same conditions. Despite being high, those values are expected since increasing mass flux also increases the friction between both phases. On the other hand, by increasing the saturation temperature, the pressure drop is slightly lower once the differences between the densities of the liquid and vapor phases are reduced. Compared with R134a, the R1234yf ecofluid presents less pressure drop, showing a reduction of 24% for 300 $kg \cdot m^{-2} \cdot s^{-1}$.

**Keywords:** R1234yf; refrigerant; pressure drop

## NOMENCLATURE

ΔP    pressure loss, kPa
G    mass flux, $kg \cdot m^{-2} \cdot s^{-1}$
g    gravitational acceleration, m/s²
GWP    Global Warming Potential
h    enthalpy, kJ/kg
I    electrical current, A
$\dot{m}$    mass flow, kg/s
ODP    Ozone Degradation Potential
$\dot{Q}$    heat rate, W
$v$    specific volume, m³/kg
V    voltage, V
x    quality

### Greek symbols

α    void fraction
θ    angle between the liquid and the horizontal
η    efficiency
$\rho$    density, kg/m³

### Subscripts

l    liquid
lg    difference between liquid and vapor
out    output
v    vapor

## INTRODUCTION

Refrigerants are constantly being replaced throughout history. Until the 1920s, natural refrigerants were used, such as propane (R290) and ammonia (R717). However, since they have high levels of toxicity and flammability, these fluids have become unfeasible for residential applications. The second generation of refrigerants was marked by substances that presented considerable safety and durability (Calm, 2008). However, due to the presence of chlorine atoms in its molecular structure, it was discovered that the use of these fluids depleted the ozone layer.

Therefore, several conferences were held. In response to the Montreal Protocol (U. N.

Environment, 1987), in the late 1980s, the use of hydrofluorocarbons (HFCs) began, which have low Ozone Degradation Potential (ODP). Among the HFCs, R134a can be mentioned as being one of the most used, until today (McLinden et al., 2014). However, even having zero ODP, such fluids have a High Global Warming Potential (GWP) and, consequently, contribute to promoting climate changes to the planet due to the intensification of the greenhouse effect.

Due to global warming considerations, the European Union has decided to ban, since January 1, 2017, the use of refrigerants with a GWP greater than 150 in new passenger cars, as well as the use of refrigerants with a GWP greater than 750 in new fixed units (E. UNION, 2006). The search for new ecological refrigerants with zero ODP and low GWP started. In this context, refrigerant R1234yf, from the family of hydrofluorolefins, was produced. This fluid has a very low GWP, zero ODP and thermodynamic properties similar to those of R134a (Tanaka et al., 2010), even with low flammability, its use is feasible in automotive systems because in these there are already highly flammable fluids and in greater quantity, therefore, it can be considered its potential operating niche. Thus, R1234yf is currently being studied as a potential replacement for R134a in automotive systems. However, more research is needed on its behavior in refrigeration systems, including studies related to pressure drop in the tubes.

With the change in the void fraction, the pressure drop increases due to the reduction in differences in the density of the vapor and liquid phases and the consequent increase in shear between them. There are correlations to estimate the void fraction, among which one can mention the Homogeneous model (Collier, 1972), the Zivi (1964) correlation, and the Hugmark (1965) correlation. A direct relationship is observed between a fluid's quality and the void fraction in the tube. So, the objective of this work is to determine how the change in the void fraction affects the pressure drop for the ecofluid R1234yf compared to the R134a for different saturation temperatures, different mass flux, and across the quality field.

In the next chapter, the experimental setup used will be presented, in sequence, the test section will be better detailed, in the results section, it will be presented how the pressure drop of the R1234yf behaves as a function of the change in the void fraction at the exit of the test section, as well as due to changes in mass fluxes and fluid saturation temperatures, compared to R134a.

**EXPERIMENTAL SETUP**

Figure 1 shows a schematic of the experimental setup build in this project that was used to obtain measurements that allowed the calculation of pressure drop in the duct of 4.8 mm of diameter. The

R134a and R1234yf fluid flows in a controlled manner, and through measurements at the condenser inlet and heating section, the fluid quality could be precisely determined.



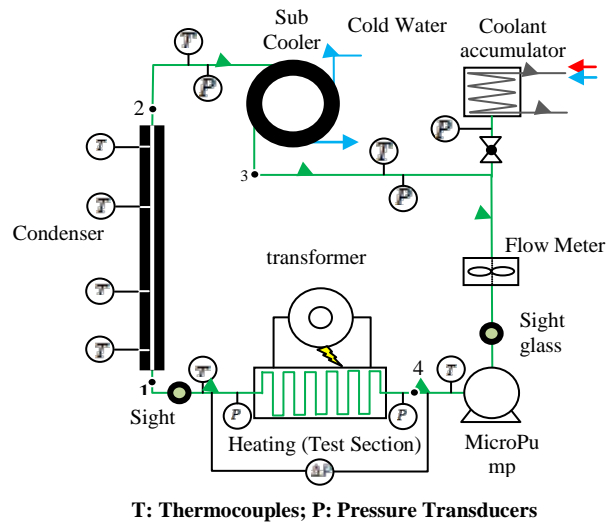**T: Thermocouples; P: Pressure Transducers**

Figure 1. Schematic representation of the built experimental setup.

The micro-pump, model GJ-N23 manufactured by Micropump, pumps the fluid in the system, through a 4.8 mm internal diameter copper tube towards the heating section, which is comprised of an electrical resistor wound around a similar copper tube, and insulated from the surroundings in thick Rockwool. In this heating section, which is analogous to an evaporator in common refrigeration cycles, the phase of the fluid change, going from liquid to vapor, this is the test section. The rate of phase change is controlled by managing the heat dissipation in the electrical resistance through a variable autotransformer. At the inlet and outlet (4 and 1, respectively), temperature and pressure are measured, and at the outlet, a sight glass is installed to visually inspect the flow conditions.

After leaving the test rig heating section, the now two-phase fluid flow enters the condenser. It consists of a concentric tube counter-current heat exchanger, in which the fluid flows through the inner tube, and the outer uses cold water to remove energy from the refrigerant. This way, as the refrigerant flows through the condenser, it condensates. Thermocouples are installed at the water inlet and outlet, as well as along the inner tube external wall. This way, temperatures are used to determine heat flow.

Upon leaving the test section, the refrigerant fluid enters the sub-cooler, whose function is to ensure complete condensation, followed by a fluid divergence valve. In this valve, fluid can either continue flowing through the test rig or be directed to an accumulator, changing the total fluid mass in the system. This is only used when setting experiments up, and not during regular test operation.

Following this divergence, the fluid flow rate is measured at the mass flux meter, a turbine type of manufacturer Kobold, pass through another sight glass to finally return to the micropump, closing the loop, and restarting operation. In Tab. 1, a summary of the components instruments is presented.

Table 1. Summary of the components.

| Sym. | Name | Description | Accuracy |
|------|------|-------------|----------|
| T | Thermocuple | Type T | ±0.35 |
| P | Pressure Transmitter | Out signal 4-20 mA | ±2kPa |
| MP | Micro pump | GJ-N23 | N/A |
| ΔP | Differential Pressure | Rosemount | ±2kPa |
| FM | Flow meter | Kobold Model | ±1.5% FS |
| W | Power meter | Oscilloscope | ±3% RD |

The acquired experimental data and each instrument accuracy were considered to calculate the expanded uncertainty for indirect measurements and calculated variables, namely mass flux, vapor quality, and HTC through Taylor (1997) proposed methodology. The instruments signals output was read through an NI USB 6211 module and a Labview test platform, specifically built to interpret signal incoming from the test rig. The data was then exported to the Engineering Equation Solver (EES) software.

**TEST SECTION (HEATING SECTION)**

The test section illustrated in Fig. 2, consists of a copper tube with an internal diameter of 4.8 mm and a length of 12.2 meters. The tube was conditioned in 20 straight sections of approximately 54 cm and 20 curves with a curvature radius of 2.4 cm. Its entire length was surrounded by a total electrical resistance of 16.1Ω, providing a maximum power of about 2.7 kW, evenly distributed over the length of the tube. The set is externally insulated with fiberglass blankets and polyurethane insulating plates, and packaged in a wooden container. Due to the geometric distribution of the electrical resistance around the tube, it is considered that the power supplied to the fluid is distributed homogeneously throughout the length of the test section.

$$X_{out} = \frac{\dot{Q} \cdot \dot{m}^{-1} - h_l + h_e}{h_{lg}} \qquad (1)$$

$$\dot{Q} = \eta \cdot V \cdot I \qquad (2)$$

A ±2kpa accuracy differential pressure meter from the Rosemount manufacturer was installed to measure the pressure drop between the input and output of the test section. The refrigerant enters the test section in the liquid phase, receives energy, and becomes two-phase with a known quality at the outlet.

This parameter, $X_{out}$, can be calculated using energy balance considering an efficiency factor $\eta$ of 0.93, which was measured experimentally, as presented in Eqs. (1) and (2), where $\dot{Q}$ is the power provided to the refrigerant in kW; $\dot{m}$ is mass flow that was measured by a flow meter from Kobold manufacture, model DPM-1153N2L443 (±1.5% FS and full-scale is equal to 0.28 gph); the enthalpies of inlet $h_l$ and outlet $h_{out}$ were calculated as a function of temperature and pressure measured with calibrated thermocouples and pressure transmitters, kJ/kg; and the vaporization enthalpy was calculated as a function of temperature of the two-phase fluid, kJ/kg.

Equation 2 calculates $\dot{Q}$, as a function of Voltage (V); in V; and current (I), in A, which are measured by oscilloscope from the Minipa manufacturer model MVBDSO (3% uncertainty over the reading).

$$\alpha = \frac{1}{1 + \left(\frac{1 - x_{out}}{x_{out}}\right) \cdot \left(\frac{\rho_v}{\rho_l}\right) \cdot \left(\frac{\rho_l}{\rho_v}\right)^{\frac{1}{3}}} \qquad (3)$$

With the output quality given by Eq. (1) and knowing the fluid outlet temperature of the test section, it is possible to determine the densities of both the liquid ($\rho_l$) and vapor ($\rho_v$) phases and in this way calculate the void fraction using the Zivi (1964) correlation, as presented in Eq. (3), where α is the void fraction; and $\rho_l$ and $\rho_v$ are given in kg/m³.
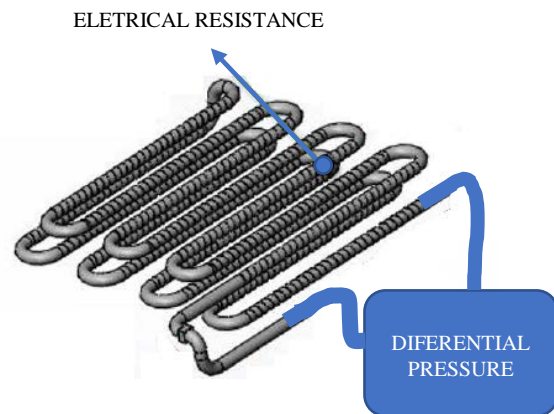


Figure 2. Schematic of Internal Test section.

**RESULTS AND DISCUSSION**

The pressure drop values in the test section were measured experimentally. With the temperature and pressure measured at the exit of the test section, it was possible to calculate the quality using Eq. (1) and subsequently, the void fraction using Eq. (3). The greater the void fraction at the outlet of the test

section, the greater is the length of the duct in which refrigerant travels through as two-phase regime, in this way, the total pressure drop suffered, the sum of both, in single and two-phase regime, is plotted in Figs. 3 and 4 Varying the saturation temperatures, mass velocities, and void fraction.

$$\frac{dP}{dz} = \left(\frac{dP}{dz} \cdot F\right) - G^2 \cdot \frac{d}{dz}\left[\frac{x_{out}^2 \cdot v_v}{\alpha} + \frac{(1-x_{out})^2 \cdot v_l}{(1-\alpha)}\right] \quad (4)$$
$$-g \cdot sen(\theta) \cdot \left[\alpha \cdot \rho_v + (1-\alpha) \cdot \rho_l\right]$$

Where G is the mass flux, $kg \cdot m^{-2} \cdot s^{-1}$, $x_{out}$ is the test section's output quality; $\alpha$ is the void fraction; $v_l$ is the specific volume of the fluid in the liquid phase, $m^3/kg$; $v_v$ is the specific volume fluid in the vapor phase, $m^3/kg$; g is the acceleration of gravity, $m/s^2$; $\theta$ is the angle between the fluid and the horizontal; $\rho_v$ is the density of the fluid in the vapor phase, $kg/m^3$; and $\rho_l$ is the density of the fluid in the liquid phase, $kg/m^3$.
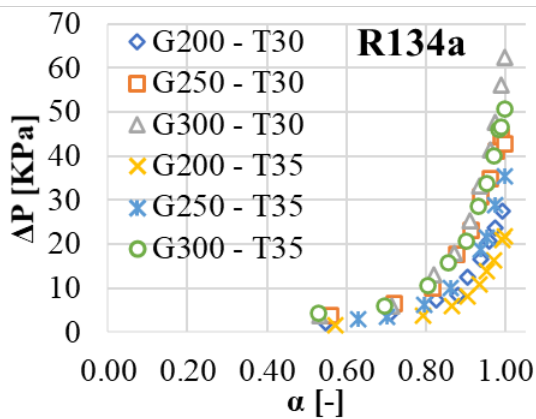


Figure 3. Pressure drop in function of the void fraction – R134a.
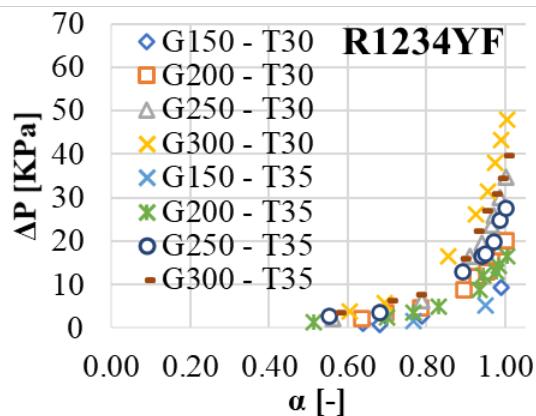


Figure 4. Pressure drop in function of the void fraction – R1234yf.

As previously stated, the pressure drop measured was plotted as a function of the void

fraction at the exit of the test section for both the R134a and R1234yf refrigerant. As presented in Eq. (4), the pressure drop in the two-phase regime can be divided into accelerational, frictional, and gravitational parts. The first term of the expression corresponds to pressure loss ($\Delta P$) due to acceleration of the fluid, the second term due to friction both with the pipe and between the liquid and vapor layers, and the third term refers to the loss of pressure due to overcoming gravitational effects.

Part of the pressure drop due to friction is a function of the shear which occurs due to the speed differences between the liquid and vapor phases. Therefore, when the saturation temperature is raised from 30 to 35ºC, the difference between the density of the liquid and vapor phases reduces 2.48%, which results in a small reduction in pressure drop.

The mass flux considerably influences the pressure drop due to friction, as shown in Eq. (4). So, the higher the mass flux, the greater the pressure drop in the tube. Tab. 2 shows an average of the pressure drop made over the entire void fraction range for the mass velocities of 200, 250, and 300 $kg \cdot m^{-2} \cdot s^{-1}$ for both temperatures of 30ºC and 35ºC and both fluids.

Table 2. Mean pressure drop for mass flux and saturation temperature.

| R1234yf | | | R134a | | |
|---|---|---|---|---|---|
| G | T30 | T35 | G | T30 | T35 |
| 200 | 11.75 | 8.69 | 200 | 12.56 | 11.01 |
| 250 | 19.64 | 16.74 | 250 | 26.89 | 14.47 |
| 300 | 28.75 | 22.21 | 300 | 29.32 | 28.75 |

As for the R1234yf, considering the data in the Tab. 2, it is possible to verify that there is an increase in the pressure drop of 144.72% when the mass speed changes from 200 to 300 $kg \cdot m^{-2} \cdot s^{-1}$ at a temperature of 30ºC. Similarly, however, at a temperature of 35ºC, the pressure drop increases 155.46% for the same change in mass flux. It is observed that even if the increase in temperature provides less pressure drop, this effect is negligible when compared to the effect of the change in mass flux.

Regarding R134a, when the mass flux was varied from 200 to 300 $kg \cdot m^{-2} \cdot s^{-1}$ at a temperature of 30ºC, there was an increase in pressure drop of 133.46%. As for the temperature of 35ºC, when it varies from 200 to 300 $kg \cdot m^{-2} \cdot s^{-1}$ the pressure drop increases by 161.07%. These increases were expected and consistent, since the higher the mass flux, the more turbulent the flow becomes and, consequently, the greater the fraction of friction with the tube and between the liquid and steam phase.

Looking at Figs. (3) and (4), it can be seen that the refrigerant R1234yf has a maximum pressure drop was close of 50 kPa at a mass speed of 300 $kg \cdot m^{-2} \cdot s^{-1}$ while R134a presents the maximum pressure drop load of 62 kPa at the same mass flux. A reduction of 24%. For other mass flux values, the

R1234yf refrigerant also showed lower pressure loss values. Juan et al. (2020) also found that R1234yf exhibits this behavior when compared to R134a.

## CONCLUSIONS

Small changes in values of low quality lead to considerable changes in the void fraction. The more two-phase the fluid is inside the tube, the greater is the pressure drop. The total pressure drop in the tube considering the sum of both the portion that flowed single-phase and the two-phase portion, was plotted as a function of the void fraction calculated at the exit of the test section for both the R134a and R1234yf fluids as showed in Figs. (3) and (4). The pressure drop was measured as a function of the mass flux of 150, 200, 250,300 kg·m$^{-2}$·s$^{-1}$for the R1234yf and 200, 250, and 300 kg·m$^{-2}$·s$^{-1}$ for R134a. Two saturation temperatures were experienced at the exit of the test section: 30ºC and 35ºC.

Regarding the increase in the saturation temperature, there is a slight reduction in the pressure drop for the same flow conditions, approximately 2.8%. This is because of the reduction in the differences in the densities of the liquid and vapor phases and the consequent reduction in the interfacial friction between them.

The increase in mass flux causes a high increase in the pressure drop imposed on the fluid. Being that for saturation temperatures at the exit of the test section of both 30ºC and 35ºC an increase in mass flux by 100 kg·m$^{-2}$·s$^{-1}$ causes an increase in the mean pressure drop by more than 100%.

Comparing the refrigerants R134a and R1234yf it is observed that the R1234yf presents lower values of pressure drop for the mass flux values studied. Considering that the maximum values assumed at the mass flux of 300 kg·m$^{-2}$·s$^{-1}$ the difference between R1234yf and R134a reaches 24%.

## ACKNOWLEDGEMENTS

## REFERENCES

Calm, J. M., 2008, The Next Generation of Refrigerants – Historical Review, Considerations, and Outlook, International Journal of Refrigeration, Vol. 31, No. 7, pp. 1123-1133.

Collier, J. G., 1972, *Convective Boiling and Condensation*, McGraw-Hill.

Union, E., 2006, Directive 2006/40/ec of the European Parliament and of the Council of 17 May 2006 Relating to Emissions from, Bruxelas.

Hughmark, G. A., 1965, Holdup and Heat Transfer in Horizontal Slug Gas-Liquid Flow, Chemical Engineering Science, Vol. 20, No. 12, pp. 1007-1010.

Juan, J. G. P., Khosravi, A., Belman-Flores, J. M., Machado, L., and Revellin, R., 2020, Applications of Refrigerant R1234yf in Heating, air Conditioning and Refrigeration Systems: a Decade of Researches, International Journal of Refrigeration, doi: https://doi.org/10.1016/j.ijrefrig.2020.06.014.

McLinden, M. O., Kazakov, A. F., Brown, S., and Domanski, P. A., 2014, A Thermodynamic Analysis of Refrigerants: possibilities and Tradeoffs for Low-GWP Refrigerants, International Journal of Refrigeration, Vol. 38, pp. 80-92.

Tanaka, K., Higashi, Y., and Akasaka, R., 2010, Measurements of the Isobaric Specific Heat Capacity and Density for HFO-1234yf in the Liquid State, Journal of Chemical & Engineering Data, Vol. 55, No. 2, pp. 901-903.

Taylor, J. R., 1997, *An Introduction to Error Analysis: the Study of Uncertainties in Physical Measurements*, Vol. 2, University Science Books.

Zivi, S. M., 1964, Estimation of Steady-State-Steam Void-Fraction by Means of the Principle of Minimum Entropy Production, Journal of Heat Transfer, Vol. 86. No. 2, pp. 247-251.